Narrow-Band-Gap-HBT Technology for Low-Power, High-Speed Applications

C. Monier, A. Cavus, R. S. Sandhu, M. D. Lange, P. Cheng, B. Chan, D. J. Sawdai,
P. C. Chang, V. F. Gambin, B. Oyama, T.R. Block, and A. L. Gutierrez-Aitken

Northrop Grumman Space Technology, Redondo Beach, CA 90278
e-mail: cedric.monier@ngc.com, Tel: (310) 812-6129

KEYWORDS: HBT, InAlAs/InGaAs, metamorphic, high indium composition, low power

Abstract

$In_xAl_{1-x}As/In_xGa_{1-x}As$ heterojunction bipolar transistors (HBTs) with indium composition of 86 % were grown on InP substrates using strain-relieved compositionally graded $In_xAl_{1-x}As$ buffers. Lattice-matched $In_{0.86}Al_{0.14}As/In_{0.86}Ga_{0.14}As$ single and double HBTs with small-emitter active areas have been fabricated on 6.0 Å graded buffer layers. Despite the use of this narrow-band-gap material system, practical breakdown voltages approaching 4 V have been demonstrated from DHBT structures with high DC gain, limited leakage at the device junctions and turn-on voltage reduction by a factor of two compared to existing InP bipolar technology. A peak cutoff frequency of 170 GHz has been measured from 6.0 Å single HBTs with 1x5 μm^2 emitter size at very low collector-emitter voltage V_{CE} of 0.55 V. Initial test circuits including 28 GHz dividers that dissipate half the power of InP-based HBT circuits have been successfully demonstrated.

INTRODUCTION

The $In_xGa_{1-x}As$ system with high indium content (80<x <100) has several unique advantages over InP and GaAs, such high electron mobility and large peak saturation velocity for extending the performance of electronic devices to high frequency at lower power dissipation [1,2]. In bipolar logic circuits, high-indium-content materials in the base layer, with narrow energy band gap of less than 0.5 eV, will primarily impact the device turn-on voltage V_{BE} that could be reduced by half compared to conventional III-V technologies. This directly translates to lower supply voltage and, these devices could be used as alternatives to InP-based HBTs for low power circuit applications [3,4]. Challenges with narrow-band-gap materials do exist, such as limited breakdown properties and excessive leakage current in addition to the selection of a suitable substrate. This paper discusses device technology and process integration for III-V heterojunction bipolar circuit applications, based on the high-indium-content InAlAs/InGaAs material system with its lattice parameter near that of InAs, and using a metamorphic buffer approach to accommodate its lattice parameter.

METAMORPHIC APPROACH

Among challenges associated with narrow-band-gap materials is the absence of a suitable semi-insulating wafer around 6.05 Å. InAs and GaSb substrates are available for growing epitaxial materials, but their high conductivity prevents their use for microwave applications. InAs bipolar junction transistors (BJTs) and InAsP/InAs HBTs have been demonstrated on InAs substrates with wafer removal/bonding techniques necessary for characterizing RF performance, which brings complication from a processing standpoint [5-7]. Another approach consists of using a metamorphic platform on semi-insulating InP substrates. In our case, an $In_xAl_{1-x}As$ strain-relieved buffer layer is graded from x = 0.52 towards InAs (x=1) to obtain lattice constants that are not presently available [8-11]. This approach offers the possibility of using any lattice parameter between InP and InAs for innovative HBT band-gap engineering, where single and double HBT designs can be lattice-matched on any given platform.

Strain-relieving misfit dislocations generated during the metamorphic buffer growth (which is utilized to accommodate the large epilayer/substrate lattice misfit) lead to the formation of a surface crosshatch pattern. The high density of threading dislocations and crosshatch features at the wafer surface could severely impact the manufacturing of integrated circuits. Growth optimization was employed to produce metamorphic buffers with low threading dislocation density (high 10^5 cm^{-2}) while minimizing surface roughness [12]. $In_xAl_{1-x}As$ buffers, compositionally graded in three continuous steps, were grown on (100) semi-insulating InP substrates using solid-source MBE. InAlAs was chosen over InGaAs because of its larger thermal conductivity. The total buffer layer was limited to 1 micron thickness to minimize thermal effects.

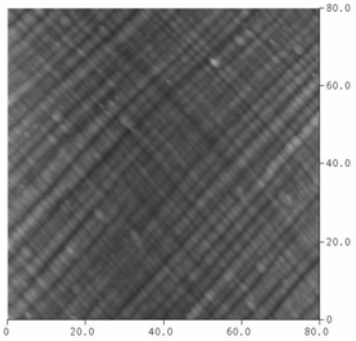

Fig. 1. AFM image from the surface of a $In_xAl_{1-x}As$ metamorphic buffer graded in three steps (grown on InP substrate) terminating with 86 % Indium. The scan area is 80 µm x 80 µm.

Fig. 1 shows an AFM image of the typical cross-hatch pattern morphology observed at the surface of metamorphic, fully-relaxed buffers. RMS roughness values of <5 nm were consistently observed.

HETEROJUNCTION BIPOLAR TRANSISTOR DESIGN

This virtual substrate approach opens the possibility of producing any desired lattice parameters between InP (5.8687 Å) and InAs (6.0585 Å). The HBT device structure developed in our approach is based on the InAlAs/InGaAs material system. The base material is made from $In_xGa_{1-x}As$ ternary material with band gap energy potentially as low as 0.35 eV. The ultimate situation with 100 % indium was not selected because only InAs lattice-matched bipolar junction transistors (BJTs) can be grown on this platform [13]. In order to take advantage of a heterojunction design at the base-emitter interface, InAlAs emitter layers would have to be grown pseudomorphically (with tensile strain) on the InAs base, and this could severely impact reliability. To avoid strain effects in the HBT structure, a lattice-matched heterojunction designed for low turn-on voltage utilizes an indium composition as close to 100% as possible while still retaining a sufficiently large valence band offset relative to the base material. The $In_xAl_{1-x}As/In_xGa_{1-x}As$ material system using 86% indium (6.0 Å) seems to present a good compromise by providing high electron mobility and saturation velocity while maintaining a low turn-on voltage. This HBT material system offers a favorable band alignment, with conduction and valence band offset values of 140 and 60 meV, respectively, as shown on Figure 3 (shown alongside the traditional InP-based HBT line-up). This system still provides significant low operating voltage with an band-gap energy in the $In_{0.86}Ga_{0.14}As$ base of 0.45 eV, which is 40% below the energy band gap of the $In_{0.53}Ga_{0.47}As$ in lattice-matched InP HBTs.

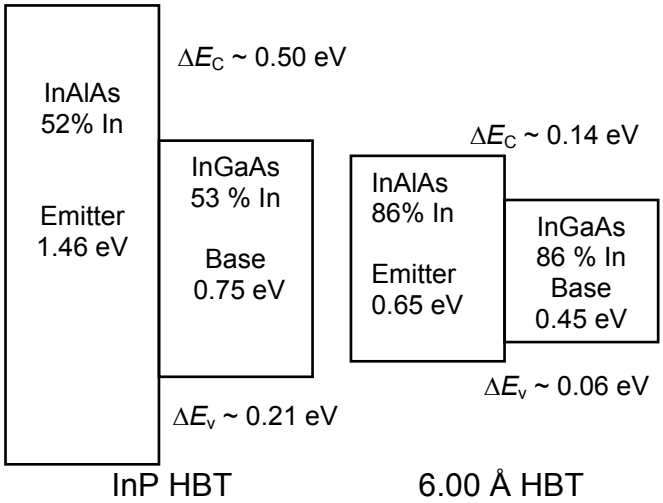

Fig. 2. Band line-up comparison between an InP-based HBT and this narrow-band-gap HBT material systems.

Table 1 shows the schematic 6.0 Å HBT epitaxial structure grown using the $In_{0.86}Al_{0.14}As/In_{0.86}Ga_{0.14}As$ material system. The base layer thickness is 400 Å thick, with 2e19 cm^{-3} Be doping concentration, and is followed by a linearly-graded base-emitter interface. The structure terminates with high-indium-composition layers that are beneficial for low emitter resistance. The 2000 Å collector layer can be either $In_{0.86}Ga_{0.14}As$ for a single HBT design or $In_{0.86}Al_{0.14}As$ for a double HBT design (with particular care given at the collector-base interface to minimize current blocking). The double-HBT design is desired to improve breakdown voltage; which is, by definition, low for narrow-band-gap materials.

TABLE 1
Schematic of 6.0 Å HBT epitaxial structure

Cap: $In_{0.86}Ga_{0.14}As$ (1e19 – Si)
Emitter: $In_{0.86}Al_{0.14}As$ (5e17 – Si)
Base: 400 Å $In_{0.86}Ga_{0.14}As$ (2e19 – Be)
Collector: 2000 Å $In_{0.86}Ga_{0.14}As$ ($In_{0.86}Al_{0.14}As$ if DHBT)
Sub-Coll.: 4000 Å $In_{0.86}Ga_{0.14}As$ ($In_{0.86}Al_{0.14}As$ if DHBT)
1 μm Graded InAlAs buffer (undoped)
SI InP Substrate

DEVICE FABRICATION

Small area devices were fabricated using most of the NGST standard InP HBT front-side and back-side processes, with minor wet-etch process changes [14]. In order to ensure good isolation for the metamorphic bipolar transistors, the isolation etch was extended into the InAlAs graded buffer layer, resulting in a much taller isolation mesa compared to traditional InP technology. One major difference from the InP production process was the use of bizbenzocyclobutene (BCB) for device passivation in replacement of the dielectric conventional SiN, with leakage reduction by 3 to 4 orders of magnitude typically observed compared to SiN. The use of this planar polymer to encapsulate the active devices necessitated an additional etch step to remove the dielectric elsewhere for the passive elements, including 20 and 100 Ω/□ NiCr thin-film resistors and MIM capacitors. Two layers of gold with airbridge crossovers were used for circuit interconnects. Devices with emitter width of 1.5 μm were used in the first generation of test circuits. Devices with narrower emitter width of 1 μm were also fabricated as test vehicles to characterize RF performance of the 6.0 Å technology.

DEVICE CHARACTERISTICS

Figure 3 exhibits the Gummel plots of small area (1.5x4 μm^2) double-HBT devices from the InP and 6.0 Å technologies. This comparison clearly shows that the turn-on voltage (the base emitter voltage needed to achieve a certain

amount of output current) is reduced by almost half by the use of a narrow-band-gap approach compared to the lattice-matched InP technology. Very similar base and collector ideality factors are observed on the 6.0 Å HBTs when compared to InP HBTs, indicating good material quality. The 6.0 Å device with a 400 Å base exhibits a DC gain β near 40. Leakage currents measured at both junctions (shown in Figure 4) confirm the effectiveness of BCB on surface passivation for narrow-band-gap materials. Reverse collector-base leakages around 10-100 nA are typically observed in the range of operating bias intended for this low-power technology (0 to -0.25V V_{CB}). Figure 5 displays the common-emitter IV characteristics of a 1.5x4 μm^2 6.0 Å HBT. No indication of current blocking is evident up to 400 kA/cm^2. Despite the narrow-band-gap collector, useful off-state breakdown voltages BV_{CE0} approaching 4 V (shown in the inset) are commonly measured. A 40 % reduction of the knee voltage is observed with InP-based HBTs of equivalent size.

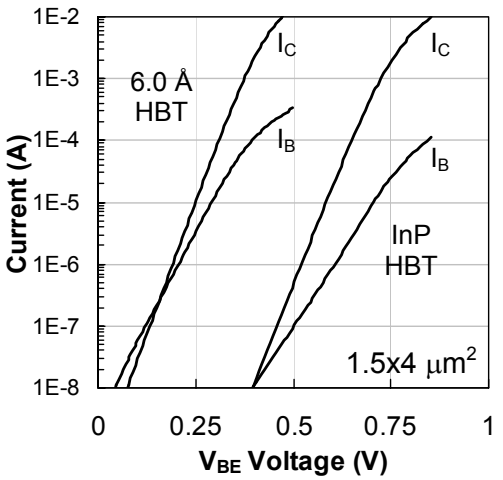

Fig. 3 Gummel-plot comparison between an InP-based HBT and an $In_xAl_{1-x}As/In_xGa_{1-x}As$ narrow band gap HBT using 86 % indium (6.0 Å)

RF measurements have been conducted on both single and double 6.0 Å HBTs. RF calibration was not done on-wafer. The cut-off frequency f_T is plotted versus the collector current density in Figure 7 for both SHBT and DHBT devices with emitter areas of 1x5 μm^2. The base-collector bias is set to 0.1 V. The SHBT design exhibits a peak frequency f_T of 170 GHz, while the double 6.0 Å HBTs shows a peak frequency at 150 GHz. A very small degradation of RF performance by 10 GHz is observed without applying any voltage at the base-collector junction (V_{CE} = V_{BE} = 0.44 V only). The maximum oscillation frequency f_{MAX} exceeds 100 GHz. This is currently limited to the base doping in the 400 Å $In_{0.86}Ga_{0.14}As$ base set to 2e19 cm^{-3} with base sheet resistance around 1200 Ω/□. Improvement is expected as more p-type dopants are incorporated. The narrow-band-gap approach compares favorably with competing technologies (InP and SiGe) in terms of power density (I_C × V_{CE}/emitter area) versus frequency. 6.0 Å HBTs exhibit the highest frequency at the lowest power density within the 50-150 GHz frequency range.

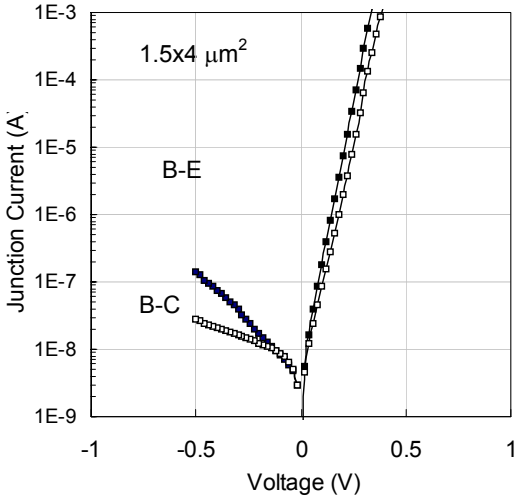

Fig. 4. Leakage current measured at collector-base and base-emitter junctions from a 1.5x4 μm^2 narrow-band-gap HBT.

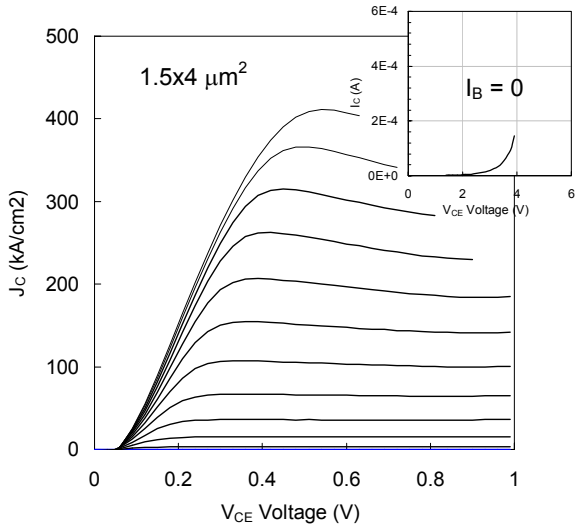

Fig. 5. Typical common-emiter IV characteristics of a 1.5x4 μm^2 6.0 Å DHBT ($I_{B\ STEP}$ = 50 μA)

CIRCUIT RESULTS

Test circuits have been designed and fabricated with 6.0 Å HBTs to demonstrate the basic building blocks needed for digital ICs. The typical number of devices per chip is in the range of 50-100 with emitter sizes of 1.5x4 μm^2. Figure 7 shows the frequency response of a divide-by-2 circuit built with the 6.0 Å HBT technology operating at a maximum frequency of 28 GHz (with the associated output waveform shown in the inset). A power/per latch dissipation of 22 mW was measured (which represents half of what is needed to operate an identical InP HBT-based circuit) by reducing the power supply from 3.3 V down to 1.5 V with narrow-band-gap HBTs. Further reduction of power consumption will be obtained with the second generation of 6.0 Å HBT that utilizes sub-micron emitter sizes.

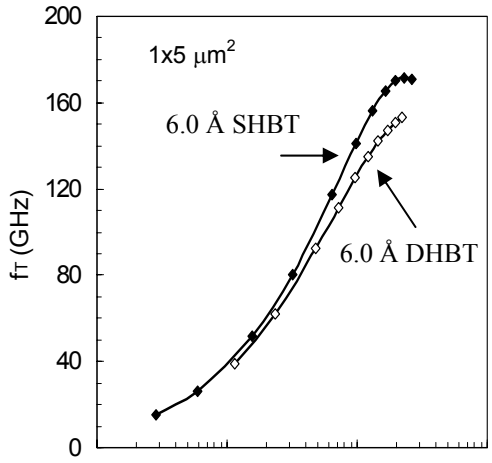

Fig.6. Cutoff frequency vs collector current density for a single (◆) and a double (◇) 6.0 Å HBT. The base-

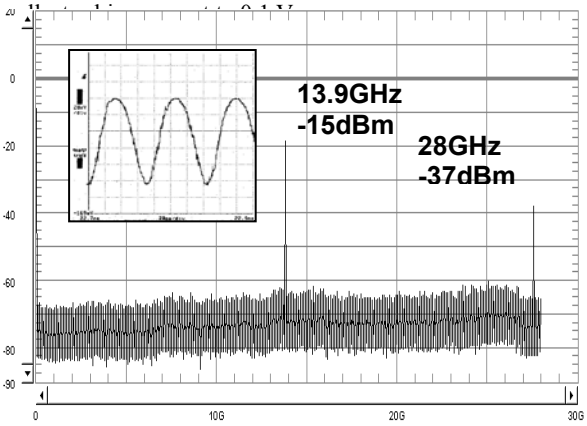

Fig. 7. Output spectrum of a divide-by-2 circuit operating at 28 GHz input frequency. The circuit uses 6.0 Å HBTs with emitter area of 1.5x4 μm^2.

CONCLUSIONS

High-indium-content $In_xAl_{1-x}As/In_xGa_{1-x}As$ single- and double-heterojunction bipolar transistors with 86% indium composition have been fabricated on InP semi-insulating substrates using a metamorphic approach. Excellent DC and RF performance was measured at very low operating voltages. Initial test circuits, including 28 GHz dividers that dissipate half the power of InP-based HBT circuits, have been successfully demonstrated. Improvements in terms of device scaling or thermal management are needed fully to develop narrow-band-gap HBTs, but these initial results show promise for reducing power consumption in future high-speed applications.

ACKNOWLEDGEMENTS

The authors would like to thank NGST engineers and technicians for their contribution to this work. This is supported by ONR Contract No. N00014-01-2-0014, DARPA ABCS program.

REFERENCES

[1] G. Satyanadh, R. P. Joshi, N. Abedin, and U. Singh, J. Appl. Phys. 91, 1331 (2002)
[2] I. Vurgaftman, J. R. Meyer, L. R. Ram-Mohan, J. Appl. Phys. 89, 5815 (2001)
[3] S. Thomas, K. Elliot, D. H. Cho, B. Shi, P. Deelman, P. Brewer, a. Arthur, R. Rajavel, C. H. Fields, and M. Madhav, Proceedings of the 2003 International Conf. on Indium Phosphide and Related Materials, pp. 26-31, May 2003.
[4] C. Monier, D. Sawdai, A. Cavus, R. Sandhu, M. Lange, J. Wang, J. Yamamoto, R. Hsing, S. Hayashi, A. Noori, T. Block. M.S. Goorsky, and A. Gutierrez-Aitken, Proceedings of the 2003 International Conf. on Indium Phosphide and Related Materials, pp. 32-36, May 2003.
[5] Maimon, K. L. Averett, X. Wu, M. W. Koch, and G. W. Wicks, IEE Electron. Lett., vol. 38, 344 (2002).
[6] P. E. Dodd, M. L. Lovejoy, M. S. Lundstrom, M. R. Melloch, J. M. Woodall, and D. Pettit, IEEE Electron Dev. Lett., vol.17, pp. 166-168, 1996
[7] S. Thomas, K. Elliott, D. H. Chow, A. Arthur, B. Shi, P. Brewer, and R. Martinez, Proceedings of the 2002 60th Device Research Conference, June 2002).
[8] H. Wang, G. I. Ng, H. Zheng, H. Yang, Y. Xiong, S. Halder, K. Yuan, C. L. Tan, K. Rahdakrishnan, and S. F. Yoon, IEEE Trans. Electron Dev., vol. 48, pp. 2671-2676, 2001.
[9] W. K. Liu, D. Lubyshev, Y. Wu, X.-M. Fang, T. Yurasits, A. B. Cornfeld, D. Mensa, S. Jaganathan, R. Pullela, M. Dahlstrom, P. K. Sundarajan, T. Mathew, and M. Rodwell, Proceedings of the 2001 International Conf. on Indium Phosphide and Related Materials, pp. 284-287, May, 2001.
[10] W. E. Hoke, P. J. Lemonias, T. D. Kennedy, A. Torabi, E. K. Tong, R. J. Bourque, J.-H. Jang, G. Cueva, D. C. Dumka, I Adesida, K. L. Chang, and K. C. Hsieh, J. Vac. Sci. Technol. B 19, 1505 (2001)
[11] Y. M. Kim, M. Dahlstrom, S. Lee, M. J. W. Rodwell, and A. C. Gossard, IEEE Electron Dev. Lett., vol. 23, pp. 297-299, 2002.
[12] M. Lange, A. Cavus, C. Monier, R. Sandhu, T. Block, V. Gambin, D. Sawdai, and A. Gutierrez-Aitken, Proceedings of the 2003 North American Conference on MBE, October 2003.
[13] D. Sawdai, C. Monier, A. Cavus, T. Block, R. Sandhu, M. S. Goorsky, A. Gutierrez-Aitken, J. Woodwall, and G. Wicks, Proceedings of the 2002 IEEE Lester Eastman Conference on High Performance Devices, August 2002).
[14] D. Sawdai, E. Kaneshiro, A. Gutierrez-Aitken, P. C. Grossman, K. Sato, W. Kim, G. Leslie, J. Eldredge, T. Block, P. Chin, L. Tran, A. K. Oki, D. C. Streit, Proceedings of the 2001 International Conf. on Indium Phosphide and Related Materials, pp. 493-496, May 2001.

ACRONYMS

SHBT: Single Hetero-junction Bipolar Transistor
DHBT: Double Hetero-junction Bipolar Transistor
BCB: bizbenzocyclobutene